



Measurement of CP violation in the decay $B^+ \rightarrow K^+ \pi^0$

LHCb collaboration[†]

Abstract

A measurement of direct CP violation in the decay $B^+ \rightarrow K^+ \pi^0$ is reported using a data sample corresponding to an integrated luminosity of 5.4 fb^{-1} , collected with the LHCb experiment at a center-of-mass energy of $\sqrt{s} = 13 \text{ TeV}$. The CP asymmetry is measured to be $0.025 \pm 0.015 \pm 0.006 \pm 0.003$, where the uncertainties are statistical, systematic, and due to an external input, respectively. This is the most precise measurement of the CP asymmetry in the decay $B^+ \rightarrow K^+ \pi^0$ and exceeds the precision on the current world average. This direct CP asymmetry is a key input to studies of a long-standing anomaly in B meson decays, known as the $K\pi$ -puzzle. The asymmetry is consistent with the previous measurements of this quantity, confirming and significantly enhancing the observed anomalous difference between the direct CP asymmetries of the $B^0 \rightarrow K^+ \pi^-$ and $B^+ \rightarrow K^+ \pi^0$ decays.

Published in Phys. Rev. Lett. 126 (2021) 091802

© 2021 CERN for the benefit of the LHCb collaboration. CC BY 4.0 licence.

[†]Full author list given at the end of the Letter.

Rare decays of heavy flavored hadrons that primarily proceed through loop-level transitions are powerful probes of the effects of new physics (NP) beyond the Standard Model (SM). The family of $B \rightarrow K\pi$ decays is dominated by hadronic loop amplitudes in the SM, but include contributions from suppressed tree-level processes, as well as electroweak loop-level processes through which NP may affect the decay [1–4]. Studies of the decay $B^0 \rightarrow K^+\pi^-$ at the B -factory experiments led to the first observation of direct CP violating asymmetries in the B system [5,6] resulting from the interference of two decay amplitudes where both the relative strong and weak phases are nonzero. The observed asymmetries in these modes are a result of the interference between tree- and loop-level amplitudes. Further studies at the B -factory and Tevatron experiments, and at LHCb have provided measurements of the branching fractions and CP asymmetries of the complete set of $B \rightarrow K\pi$ decays: $B^0 \rightarrow K^+\pi^-$ [7–10], $B^+ \rightarrow K^+\pi^0$ [8, 11], $B^0 \rightarrow K^0\pi^0$ [12, 13] and $B^+ \rightarrow K^0\pi^+$ [8, 14, 15], where the inclusion of charge-conjugated processes is implied throughout this Letter, except where asymmetries are discussed. The amplitudes in the SM are expected to obey relations imposed by isospin symmetry [1–4, 16–21]. However, measurements have revealed inconsistencies with this expectation. The largest observed discrepancy is between the measured direct CP asymmetries of the decays $B^0 \rightarrow K^+\pi^-$ and $B^+ \rightarrow K^+\pi^0$. The difference between $A_{CP}(B^0 \rightarrow K^+\pi^-) = -0.084 \pm 0.004$ and $A_{CP}(B^+ \rightarrow K^+\pi^0) = 0.040 \pm 0.021$ is nonzero at 5.5 standard deviations (σ), whereas equal asymmetries are expected based on isospin arguments. A more accurate examination of this anomaly, known as the $K\pi$ puzzle, is through the sum rule

$$A_{CP}(K^+\pi^-) + A_{CP}(K^0\pi^+) \frac{\mathcal{B}(K^0\pi^+)}{\mathcal{B}(K^+\pi^-)} \frac{\tau_0}{\tau_+} = A_{CP}(K^+\pi^0) \frac{2\mathcal{B}(K^+\pi^0)}{\mathcal{B}(K^+\pi^-)} \frac{\tau_0}{\tau_+} + A_{CP}(K^0\pi^0) \frac{2\mathcal{B}(K^0\pi^0)}{\mathcal{B}(K^+\pi^-)} \quad (1)$$

proposed in Ref. [19], where $A_{CP}(K\pi)$ and $\mathcal{B}(K\pi)$ are the CP asymmetries and the branching fractions of the $B \rightarrow K\pi$ decays and τ_0/τ_+ is the ratio of the B^0 and B^+ lifetimes. This sum rule predicts a nonzero direct asymmetry of $A_{CP}(B^0 \rightarrow K^0\pi^0) = -0.150 \pm 0.032$ using current world averages for the other quantities [22]. The current measurement of this quantity is 0.01 ± 0.10 [22]. The $K\pi$ puzzle has been the subject of significant theoretical attention, which includes more complete examination of the SM predictions as well as potential NP sources of the discrepancies [1–4, 16, 18–21].

This Letter presents a measurement of direct CP asymmetry in the decay $B^+ \rightarrow K^+\pi^0$,

$$A_{CP} = \frac{\Gamma(B^- \rightarrow K^-\pi^0) - \Gamma(B^+ \rightarrow K^+\pi^0)}{\Gamma(B^- \rightarrow K^-\pi^0) + \Gamma(B^+ \rightarrow K^+\pi^0)} \quad (2)$$

where $\Gamma(B^\pm \rightarrow K^\pm\pi^0)$ refers to the rate of $B^\pm \rightarrow K^\pm\pi^0$ decays, using data recorded with the LHCb detector at the CERN Large Hadron Collider. The data sample corresponds to an integrated luminosity of 5.4 fb^{-1} collected at a center-of-mass energy of 13 TeV between 2016 and 2018.

The LHCb detector [23, 24] is a single-arm forward spectrometer covering the pseudorapidity range $2 < \eta < 5$. The detector includes a high-precision tracking system consisting of a silicon-strip vertex detector surrounding the pp interaction region, a large-area silicon-strip detector located upstream of a dipole magnet with a bending power of about 4 Tm, and three stations of silicon-strip detectors and straw drift tubes placed downstream of the magnet. The tracking system provides a measurement of momentum, p , of charged particles with a relative uncertainty that varies from 0.5% at low momentum

to 1.0% at 200 GeV/ c . The minimum distance of a track to a primary pp collision vertex (PV), the impact parameter (IP), is measured with a resolution of $(15 + 29/p_T)$ μm , where p_T is the component of p transverse to the beam, in GeV/ c . Different types of charged hadrons are distinguished using information from two ring-imaging Cherenkov detectors (RICH). Photons, electrons and hadrons are identified by a calorimeter system consisting of scintillating pad and preshower detectors, an electromagnetic and a hadronic calorimeter. Charged and neutral clusters in the electromagnetic calorimeter (ECAL) are separated by extrapolating the tracks reconstructed by the tracking system to the calorimeter plane, while photons and neutral pions are distinguished by cluster shape and energy distributions.

Simulated events are used to model the effects of the detector acceptance and the imposed selection requirements. In the simulation, pp collisions are generated using PYTHIA [25] with a specific LHCb configuration [26]. Decays of unstable particles are described by EVTGEN [27], in which final-state radiation is generated using PHOTOS [28]. The interaction of the generated particles with the detector and its response are implemented using the GEANT4 toolkit [29] as described in Ref. [30].

The decay topology $B^+ \rightarrow h^+\pi^0$, where h^+ is a charged hadron, presents a unique challenge in the proton-proton collision environment of the LHC. These decays comprise a single charged track and lack a reconstructible displaced vertex, a signature typically used to identify the decays of b hadrons. The candidate selection for $B^+ \rightarrow K^+\pi^0$ candidates instead relies on identifying a charged kaon that is inconsistent with originating from any PV but consistent with originating from the B -meson trajectory. That trajectory is determined by adding the momenta of the K^+ and π^0 candidates, where the π^0 momentum is defined as pointing from the LHCb interaction point to the coordinate of the energy deposited by the π^0 candidate in the calorimeter.

The LHCb trigger system [31] consists of a hardware stage, based on information from the calorimeter and muon systems, followed by a software stage, in which a full event reconstruction is applied. Events are required to pass a hardware trigger that selects a neutral pion or photon with a high transverse energy based on energy deposits in the calorimeter. Because of the limited ECAL position resolution a significant fraction of high p_T $\pi^0 \rightarrow \gamma\gamma$ decays have their photons merged into a single cluster. Only this π^0 category is used in this analysis, as neutral pions with the photons resolved suffer from a large background of randomly combined clusters. Further selection relies on a dedicated software trigger developed for this analysis [32]. A $B^+ \rightarrow K^+\pi^0$ candidate is formed by adding the four-momenta of the neutral pion and a charged track identified as a kaon using information from the RICH detectors. The charged kaon is required to have $p > 12$ GeV/ c , $p_T > 1.2$ GeV/ c , and a significant IP with respect to any PV. The neutral pion is required to have $p_T > 3.5$ GeV/ c and the scalar sum of the K^+ and π^0 p_T must exceed 6.5 GeV/ c . The B^+ candidate is required to have a $K^+\pi^0$ invariant mass in the range $4 \leq m(K^+\pi^0) \leq 6.2$ GeV/ c^2 , and $p_T > 5$ GeV/ c . Finally, the B^+ candidate trajectory is obtained by fixing its momentum vector to the PV with the smallest kaon IP. The significance of the distance of closest approach between the K^+ candidate and this trajectory is denoted as DOCA- χ^2 . In order to identify K^+ candidates consistent with production via B -meson decay, the DOCA- χ^2 is required to be small. In the offline reconstruction, a stricter set of particle identification requirements are applied to the K^+ candidates.

Further candidate selection is based on variables characterizing how well isolated a

candidate is from other tracks in the event. Vertex-isolation variables are calculated by combining each track in the event with the K^+ candidate individually to form a two-track secondary vertex. Three related variables are calculated: the smallest χ^2 of the vertex fit between the K^+ and any other track, the smallest change in χ^2 when one more track is added to that vertex, and the multiplicity of vertices having small χ^2 . The isolation of the candidate is also measured with the p_T asymmetry

$$\mathcal{A}(p_T) = \frac{p_{T_B} - p_{T_{\text{cone}}}}{p_{T_B} + p_{T_{\text{cone}}}}, \quad (3)$$

comparing the transverse momentum of the B^+ candidate (p_{T_B}) to a scalar sum of additional charged particles nearby ($p_{T_{\text{cone}}}$). Particles are considered in a cone around the reconstructed B^+ trajectory with a radius in the η - ϕ plane of $\Delta R \equiv \sqrt{(\Delta\phi)^2 + (\Delta\eta)^2} = 1.7$, where $\Delta\phi$ is the difference in radians between the azimuthal angles of the momentum of the reconstructed B^+ candidate and the track, and $\Delta\eta$ is the difference between their pseudorapidities. To ensure that the simulated distributions of these variables for the signal decays are consistent with data, candidate weights are generated from the ratios of these distributions between simulated $B^0 \rightarrow K^+\pi^-$ decays and a control sample of $B^0 \rightarrow K^+\pi^-$ candidates selected in the same data set. A gradient boosted reweighter (GBR) [33] technique is used to determine the weights, which are subsequently applied to the $B^+ \rightarrow K^+\pi^0$ simulations.

The final candidate selection is performed using boosted decision tree (BDT) classifiers with the isolation variables, the DOCA- χ^2 , the smallest change in χ^2 of the PV when including the K^+ track in the vertex fit, the p_T of the B^+ and the K^+ candidates, and the momentum of the π^0 candidate as inputs. These variables are chosen to provide discriminatory power between signal and background without biasing the $m(K^+\pi^0)$ distribution.

Two pairs of BDTs are trained and tested using data to represent background and simulated $B^+ \rightarrow K^+\pi^0$ decays, corrected as described above, to represent signal. One pair of BDTs is trained on background data with candidate invariant mass $m(K^+\pi^0) < 4860 \text{ MeV}/c^2$, which is dominated by partially reconstructed b -hadron decays. Another pair of BDTs is trained on background data with $m(K^+\pi^0) > 5700 \text{ MeV}/c^2$, which are primarily random $K^+\pi^0$ combinations (combinatorial background). In each of these categories, the data sample is split randomly, a BDT classifier is trained and tested on each half, and then used to assign a score to the candidates in the other half [34, 35]. This avoids biases due to artifacts in the training samples, while taking advantage of the full set of data available. The optimal requirements on the classifier response variables are found for the data set by maximizing ϵ/\sqrt{N} , where ϵ is the signal selection efficiency, evaluated on simulated events, and N is the total number of candidates observed in a region of approximately 3 times the observed $B^+ \rightarrow K^+\pi^0$ resolution around the expected B^+ mass.

Kaon candidates with $p_T > 17 \text{ GeV}/c$ or $p > 250 \text{ GeV}/c$ are removed from the sample after BDT selection because of insufficient coverage in the $B^+ \rightarrow J/\psi K^+$ control sample described below. They account for only 3% of the candidates after final selection.

The $m(K^+\pi^0)$ distribution of the selected $B^+ \rightarrow K^+\pi^0$ candidates, separated by the charge of the B meson, is shown in Fig. 1 along with the results of a fit to the data. In the fit, the signal is modeled by the sum of a Crystal Ball function [36] and a Gaussian function with an exponential tail describing the high-mass region. The Crystal Ball and

the Gaussian functions share a common mean and width that varies freely in the fit, and their tail shape parameters are fixed from simulation. Combinatorial background is modeled by an exponential function, with the exponent parameter allowed to vary freely in the fit. The tail of a Gaussian function is used to model the partially reconstructed background in the low-mass region, with mean and width allowed to vary freely in the fit. The rate of $\pi^+ \rightarrow K^+$ misidentification is measured in $D^0 \rightarrow K^-\pi^+$ decays as a function of pion momentum and pseudorapidity, with the same particle identification requirements as signal events [37]. The contribution of the misidentified $B^+ \rightarrow \pi^+\pi^0$ background is inferred from its branching fraction [38] and the misidentification rate to be 2.4% of the $B^+ \rightarrow K^+\pi^0$ yield. The $B^+ \rightarrow \pi^+\pi^0$ background component is modeled by a Gaussian with mean and resolution fixed to values determined from simulated events and a yield fixed to the expectation. There is assumed to be no asymmetry in this background.

An additional class of background candidates arises from decays such as $B^+ \rightarrow (K^{*+} \rightarrow K^+\pi^0)\pi^0$, $B^0 \rightarrow (K^{*0} \rightarrow K^+\pi^-)\pi^0$, and $B^0 \rightarrow K^+(\rho^- \rightarrow \pi^-\pi^0)$ where a pion from the K^* or ρ^- decay is not reconstructed. The polarization of the K^* or ρ^- meson results in a double peaked $m(K^+\pi^0)$ distribution, where the higher-mass peak is close to the expected B mass. This type of background is modeled with a parabolic function convolved with a Gaussian resolution function following the method described in Ref. [39]. The width of the resolution function is fixed to that of the signal resolution and the end points are fixed to the kinematic end points, allowing for a shift between the fitted and the known B^+ masses [38]. The lower-mass peak contributes below the $m(K^+\pi^0)$ range considered, and so its relative height is fixed to a value determined from simulation.

Other background sources include: $B^+ \rightarrow (K^{*+} \rightarrow K^+\pi^0)\gamma$ decays where the γ is misidentified as a π^0 ; $B^+ \rightarrow (f^0(980) \rightarrow \pi^0\pi^0)K^+$ decays where one π^0 is not reconstructed; and $B^0 \rightarrow (\bar{D}^0 \rightarrow K^+\pi^-)\pi^0$, $B^0 \rightarrow (K_0^*(1430) \rightarrow K^+\pi^-)\pi^0$ and $B_s^0 \rightarrow K^+\pi^0\pi^-$ decays where the π^- is not reconstructed. Simulation studies have shown that these background contributions either have $m(K^+\pi^0)$ distributions indistinguishable from the partially reconstructed samples described by a Gaussian tail, or in the case of $B_s^0 \rightarrow K^+\pi^0\pi^-$ has a branching fraction too small to give an observable contribution.

The data are fitted separately in four categories. In order to reduce uncertainties due to non-uniformity of the detector, candidates are separated according to whether the LHCb dipole magnetic field is aligned vertically upward (Magnet Up) or downward (Magnet Down) in the experiment. Candidates are further separated by B -meson charge in order to measure the CP asymmetry. The yield and asymmetry of each fit component are allowed to vary freely while the shape parameters are the same for the B^+ and B^- candidates. The total yield of $B^\pm \rightarrow K^\pm\pi^0$ decays is measured to be 8310 ± 255 in the Magnet Up data set and 8373 ± 253 in the Magnet Down data set. The raw asymmetry, A_{raw} , between the B^- and B^+ signal yields is found to be 0.019 ± 0.021 for Magnet Down and 0.005 ± 0.022 for Magnet Up. The results are consistent when candidates are separated by data-taking year as well as when shape parameters are allowed to vary independently for all four data categories.

As the measured asymmetry receives contributions from a number of nuisance asymmetries, the CP asymmetry can be expressed as

$$A_{CP}(B^+ \rightarrow K^+\pi^0) = A_{\text{raw}}(B^+ \rightarrow K^+\pi^0) - A_{\text{prod.}}^B - A_{\text{det.}}^K, \quad (4)$$

where $A_{\text{prod.}}^B$ is the production asymmetry of B^\pm mesons and $A_{\text{det.}}^K$ is the combined asymmetry in detection, triggering, and reconstruction of K^\pm mesons. These effects must

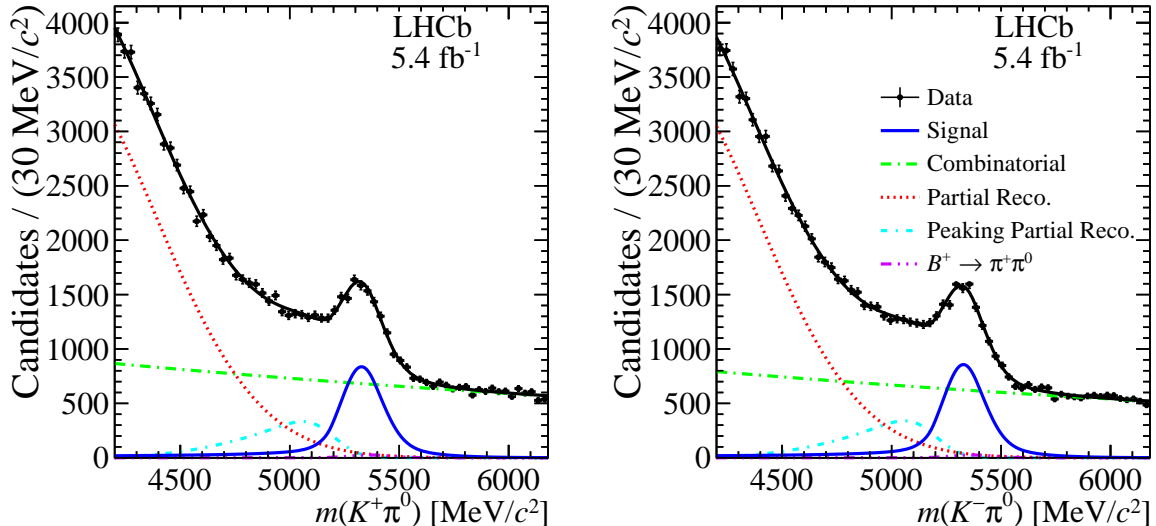


Figure 1: Invariant-mass distribution of the selected candidates with fit projections overlaid. The data set is divided by the charge of the B meson, with $B^+ \rightarrow K^+\pi^0$ shown on the left and $B^- \rightarrow K^-\pi^0$ on the right.

be corrected for in order to extract A_{CP} from A_{raw} . The combined effect of the nuisance asymmetries is measured with a control sample of $B^+ \rightarrow (J/\psi \rightarrow \mu^+\mu^-)K^+$ decays, using the same data sample as the signal channel.

In the hardware trigger, events with a $B^+ \rightarrow (J/\psi \rightarrow \mu^+\mu^-)K^+$ decay are required to trigger on particles other than the kaon, in order to avoid introducing additional trigger asymmetries. At the software stage the event must trigger on the kaon in the same manner as signal events. The offline selection requires that the B -meson lifetime be greater than 0.1 ps and that the kaon and muons have a significant IP with respect to all PVs. Additional requirements on the momentum of the kaon and B candidates as well as kaon particle identification are imposed to match the signal selection. The momentum distributions of the B^+ and K^+ candidates are weighted to match those of the signal candidates using the GBR technique [33], as the production and detection asymmetries may depend on kinematics of the decay.

The raw asymmetry in the $B^+ \rightarrow J/\psi K^+$ signal yields is determined via an unbinned maximum-likelihood fit in which the invariant-mass distribution of the $B^+ \rightarrow J/\psi K^+$ candidates is modeled by the sum of two Gaussian functions sharing a common mean, while the combinatorial background is modeled by an exponential distribution. The total yield of $B^+ \rightarrow J/\psi K^+$ decays is measured to be 372874 ± 776 for Magnet Down and 306821 ± 699 for Magnet Up data samples with a purity of approximately 99%. The raw asymmetry is found to be -0.009 ± 0.002 for Magnet Up, and -0.012 ± 0.002 for Magnet Down samples. The CP asymmetry for the decay $B^+ \rightarrow (J/\psi \rightarrow \mu^+\mu^-)K^+$ is taken to be $A_{CP}(B^+ \rightarrow J/\psi K^+) = 0.002 \pm 0.003$ from Ref. [38]. After subtracting A_{CP} , the remaining asymmetry is attributed to the combination of production, detection, reconstruction, and triggering effects, which can then be determined from

$$A_{\text{prod.}}^B + A_{\text{det.}}^K = A_{\text{raw}}(B^+ \rightarrow J/\psi K^+) - A_{CP}(B^+ \rightarrow J/\psi K^+). \quad (5)$$

This estimate of the nuisance asymmetry is then used in Eq. 4 to determine $A_{CP}(B^+ \rightarrow$

Table 1: Systematic uncertainties on $A_{CP}(B^+ \rightarrow K^+\pi^0)$.

Systematic	Value ($\times 10^{-3}$)
Signal modeling shape	4.3
Combinatorial background shape	1.3
Partial reco. background shape	1.3
Peaking partial reco. background shape	1.2
Peaking partial reco. background offset	1.3
Peaking partial reco. background resolution	1.4
$B^+ \rightarrow \pi^+\pi^0$ yield	1.3
$B^+ \rightarrow \pi^+\pi^0$ CP asymmetry	1.5
Multiple candidates	1.3
Production/detection asymmetry stat.	2.1
Production/detection asymmetry weights	0.5
Sum in quadrature	6.1

$K^+\pi^0$). This is done separately for the Magnet Up and Magnet Down data. By averaging the Magnet Up and Magnet Down results, the direct CP asymmetry is determined to be $A_{CP}(B^+ \rightarrow K^+\pi^0) = 0.025 \pm 0.015$, where the uncertainty is statistical only.

To assess the systematic uncertainty due to mismodeling of the signal and background line shapes, pseudoexperiments are generated for variations of the $m(K^+\pi^0)$ fit model. The leading source of systematic uncertainty is from modeling the signal component in the fit. This uncertainty is assessed by replacing the default model with a single Gaussian distribution. Systematic uncertainties are assessed for numerous fit variations: replacing the exponential distribution for the combinatorial background with a linear function, individually replacing each low-mass background model with an Argus function, allowing the position and resolution of the peaking low-mass background to vary freely and independently of the signal distribution, and varying the yield and asymmetry of $B^+ \rightarrow \pi^+\pi^0$ background. Pseudoexperiments are also generated to assess the systematic uncertainty due to including events with multiple candidates in the base analysis.

The statistical uncertainty on the determination of the raw $B^+ \rightarrow J/\psi K^+$ asymmetry is also considered as a systematic uncertainty, and is the subdominant source of systematic uncertainty. Additionally, the difference between the nuisance asymmetries with and without applying the GBR weights is taken to be a systematic uncertainty. The estimated values for all systematic uncertainties are shown in Table 1, where the common value of 0.0013 is from the statistical uncertainty of the pseudoexperiments generated. The $A_{CP}(B^+ \rightarrow J/\psi K^+)$ precision of 0.003 is considered separately as an external-input uncertainty.

In conclusion, the direct CP asymmetry of the decay $B^+ \rightarrow K^+\pi^0$ has been measured with the LHCb detector using a data sample corresponding to a luminosity of 5.4 fb^{-1} . It is found to be

$$A_{CP}(B^+ \rightarrow K^+\pi^0) = 0.025 \pm 0.015 \pm 0.006 \pm 0.003,$$

where the first uncertainty is statistical, the second is systematic and the third due to external inputs, exceeding the precision of the current world average [22]. This result is consistent with the world average and consistent with zero at approximately 1.5σ .

The CP asymmetry difference, $\Delta A_{CP}(K\pi) \equiv A_{CP}(B^+ \rightarrow K^+\pi^0) - A_{CP}(B^0 \rightarrow K^+\pi^-)$, is found to be 0.108 ± 0.017 , where $A_{CP}(B^0 \rightarrow K^+\pi^-)$ is taken from Ref. [22]¹. Including the result presented in this Letter, the new world average of $A_{CP}(B^+ \rightarrow K^+\pi^0)$ is found to be 0.031 ± 0.013 . This corresponds to $\Delta A_{CP}(K\pi) = 0.115 \pm 0.014$, which is nonzero with a significance of more than 8 standard deviations, substantially enhanced over the results prior to this measurement. The updated sum rule prediction for $A_{CP}(B^0 \rightarrow K^0\pi^0)$, shown in Eq. 1, is found to be -0.138 ± 0.025 , departing from zero with a significance of approximately 5.5σ .

Acknowledgements

We express our gratitude to our colleagues in the CERN accelerator departments for the excellent performance of the LHC. We thank the technical and administrative staff at the LHCb institutes. We acknowledge support from CERN and from the national agencies: CAPES, CNPq, FAPERJ and FINEP (Brazil); MOST and NSFC (China); CNRS/IN2P3 (France); BMBF, DFG and MPG (Germany); INFN (Italy); NWO (Netherlands); MNiSW and NCN (Poland); MEN/IFA (Romania); MSHE (Russia); MICINN (Spain); SNSF and SER (Switzerland); NASU (Ukraine); STFC (United Kingdom); DOE NP and NSF (USA). We acknowledge the computing resources that are provided by CERN, IN2P3 (France), KIT and DESY (Germany), INFN (Italy), SURF (Netherlands), PIC (Spain), GridPP (United Kingdom), RRCKI and Yandex LLC (Russia), CSCS (Switzerland), IFIN-HH (Romania), CBPF (Brazil), PL-GRID (Poland) and OSC (USA). We are indebted to the communities behind the multiple open-source software packages on which we depend. Individual groups or members have received support from AvH Foundation (Germany); EPLANET, Marie Skłodowska-Curie Actions and ERC (European Union); A*MIDEX, ANR, Labex P2IO and OCEVU, and Région Auvergne-Rhône-Alpes (France); Key Research Program of Frontier Sciences of CAS, CAS PIFI, CAS CCEPP, Fundamental Research Funds for Central Universities, and Sci. & Tech. Program of Guangzhou (China); RFBR, RSF and Yandex LLC (Russia); GVA, XuntaGal and GENCAT (Spain); the Royal Society and the Leverhulme Trust (United Kingdom).

References

- [1] A. J. Buras, R. Fleischer, S. Recksiegel, and F. Schwab, *The $B \rightarrow \pi K$ puzzle and its relation to rare B and K decays*, Eur. Phys. J. **C32** (2003) 45, [arXiv:hep-ph/0309012](#).
- [2] A. J. Buras, R. Fleischer, S. Recksiegel, and F. Schwab, *$B \rightarrow \pi\pi$, new physics in $B \rightarrow \pi K$, and implications for rare K and B decays*, Phys. Rev. Lett. **92** (2004) 101804.
- [3] A. J. Buras, R. Fleischer, S. Recksiegel, and F. Schwab, *Anatomy of prominent B and K decays and signatures of cp -violating new physics in the electroweak penguin sector*, Nuclear Physics B **697** (2004) 133 .

¹The world average includes the LHCb measurement, and a small correlation between the LHCb measurements of $A_{CP}(B^0 \rightarrow K^+\pi^-)$ and $A_{CP}(B^+ \rightarrow K^+\pi^0)$ due to the charged kaon detection asymmetry has been neglected

- [4] S. Baek *et al.*, $B \rightarrow \pi K$ puzzle and new physics, Phys. Rev. **D71** (2005) 057502.
- [5] BaBar collaboration, B. Aubert *et al.*, Direct CP violating asymmetry in $B^0 \rightarrow K^+\pi^-$ decays, Phys. Rev. Lett. **93** (2004) 131801, arXiv:hep-ex/0407057.
- [6] Belle collaboration, Y. Chao *et al.*, Evidence for direct CP violation in $B^0 \rightarrow K^+\pi^-$ decays, Phys. Rev. Lett. **93** (2004) 191802, arXiv:hep-ex/0408100.
- [7] BaBar collaboration, J. P. Lees, Measurement of CP asymmetries and branching fractions in charmless two-body B-meson decays to pions and kaons, Phys. Rev. **D87** (2013) 052009, arXiv:1206.3525.
- [8] Belle collaboration, Y.-T. Duh *et al.*, Measurements of branching fractions and direct CP asymmetries for $B \rightarrow K\pi$, $B \rightarrow \pi\pi$ and $B \rightarrow KK$ decays, Phys. Rev. **D87** (2013) 031103, arXiv:1210.1348.
- [9] CDF collaboration, T. A. Aaltonen *et al.*, Measurements of direct CP-violating asymmetries in charmless decays of bottom baryons, Phys. Rev. Lett. **113** (2014) 242001, arXiv:1403.5586.
- [10] LHCb collaboration, R. Aaij *et al.*, Measurement of CP asymmetries in two-body $B_{(s)}^0$ -meson decays to charged pions and kaons, Phys. Rev. **D98** (2018) 032004, arXiv:1805.06759.
- [11] BaBar collaboration, B. Aubert *et al.*, Study of $B^0 \rightarrow \pi^0\pi^0$, $B^\pm \rightarrow \pi^\pm\pi^0$, and $B^\pm \rightarrow K^\pm\pi^0$ decays, and isospin analysis of $B \rightarrow \pi\pi$ decays, Phys. Rev. **D76** (2007) 091102, arXiv:0707.2798.
- [12] BaBar collaboration, B. Aubert *et al.*, Measurement of time dependent CP asymmetry parameters in B^0 meson decays to ωK_S^0 , $\eta' K^0$, and $\pi^0 K_S^0$, Phys. Rev. **D79** (2009) 052003, arXiv:0809.1174.
- [13] Belle collaboration, M. Fujikawa *et al.*, Measurement of CP asymmetries in $B^0 \rightarrow K^0\pi^0$ decays, Phys. Rev. **D81** (2010) 011101, arXiv:0809.4366.
- [14] BaBar collaboration, B. Aubert *et al.*, Observation of $B^+ \rightarrow \bar{K}^0 K^+$ and $B^0 \rightarrow K^0 \bar{K}^0$, Phys. Rev. Lett. **97** (2006) 171805, arXiv:hep-ex/0608036.
- [15] LHCb collaboration, R. Aaij *et al.*, Branching fraction and CP asymmetry of the decays $B^+ \rightarrow K_S^0\pi^+$ and $B^+ \rightarrow K_S^0 K^+$, Phys. Lett. **B726** (2013) 646, arXiv:1308.1277.
- [16] S. Baek and D. London, Is there still a $B \rightarrow K\pi$ puzzle?, Physics Letters **B653** (2007) 249 .
- [17] M. Ciuchini *et al.*, Searching for new physics with $B \rightarrow K\pi$ decays, Physics Letters **B674** (2009) 197 .
- [18] S. Baek, C.-W. Chiang, and D. London, The $B \rightarrow K\pi$ puzzle: 2009 update, Physics Letters **B675** (2009) 59 .
- [19] M. Gronau, A precise sum rule among four $B \rightarrow K\pi$ CP asymmetries, Phys. Lett. **B627** (2005) 82, arXiv:hep-ph/0508047.

- [20] N. B. Beaudry *et al.*, *The $B \rightarrow \pi K$ puzzle revisited*, JHEP **01** (2018) 074, [arXiv:1709.07142](#).
- [21] R. Fleischer, R. Jaarsma, and K. K. Vos, *Towards new frontiers with $B \rightarrow \pi K$ decays*, Phys. Lett. **B785** (2018) 525, [arXiv:1712.02323](#).
- [22] Heavy Flavor Averaging Group, Y. Amhis *et al.*, *Averages of b -hadron, c -hadron, and τ -lepton properties as of 2018*, [arXiv:1909.12524](#), updated results and plots available at <https://hflav.web.cern.ch>.
- [23] LHCb collaboration, A. A. Alves Jr. *et al.*, *The LHCb detector at the LHC*, JINST **3** (2008) S08005.
- [24] LHCb collaboration, R. Aaij *et al.*, *LHCb detector performance*, Int. J. Mod. Phys. **A30** (2015) 1530022, [arXiv:1412.6352](#).
- [25] T. Sjöstrand, S. Mrenna, and P. Skands, *PYTHIA 6.4 physics and manual*, JHEP **05** (2006) 026, [arXiv:hep-ph/0603175](#); T. Sjöstrand, S. Mrenna, and P. Skands, *A brief introduction to PYTHIA 8.1*, Comput. Phys. Commun. **178** (2008) 852, [arXiv:0710.3820](#).
- [26] I. Belyaev *et al.*, *Handling of the generation of primary events in Gauss, the LHCb simulation framework*, J. Phys. Conf. Ser. **331** (2011) 032047.
- [27] D. J. Lange, *The EvtGen particle decay simulation package*, Nucl. Instrum. Meth. **A462** (2001) 152.
- [28] P. Golonka and Z. Was, *PHOTOS Monte Carlo: A precision tool for QED corrections in Z and W decays*, Eur. Phys. J. **C45** (2006) 97, [arXiv:hep-ph/0506026](#).
- [29] Geant4 collaboration, J. Allison *et al.*, *Geant4 developments and applications*, IEEE Trans. Nucl. Sci. **53** (2006) 270; Geant4 collaboration, S. Agostinelli *et al.*, *Geant4: A simulation toolkit*, Nucl. Instrum. Meth. **A506** (2003) 250.
- [30] M. Clemencic *et al.*, *The LHCb simulation application, Gauss: Design, evolution and experience*, J. Phys. Conf. Ser. **331** (2011) 032023.
- [31] R. Aaij *et al.*, *The LHCb trigger and its performance in 2011*, JINST **8** (2013) P04022, [arXiv:1211.3055](#).
- [32] LHCb collaboration, *Study of the decay $B^+ \rightarrow K^+ \pi^0$ at LHCb*, LHCb-CONF-2015-001, 2015.
- [33] A. Rogozhnikov, *Reweighting with boosted decision trees*, Journal of Physics: Conference Series **762** (2016) 012036.
- [34] M. Stone, *Cross-validators: choice and assessment of statistical predictions*, Journal of the Royal Statistical Society: Series B (Methodological) **36** (1974) 111.
- [35] D. M. Allen, *The relationship between variable selection and data augmentation and a method for prediction*, Technometrics **16** (1974) 125.

- [36] T. Skwarnicki, *A study of the radiative cascade transitions between the Upsilon-prime and Upsilon resonances*, PhD thesis, Institute of Nuclear Physics, Krakow, 1986, DESY-F31-86-02.
- [37] L. Anderlini *et al.*, *The PIDCalib package*, LHCb-PUB-2016-021, 2016.
- [38] Particle Data Group, P. A. Zyla *et al.*, *Review of particle physics*, Prog. Theor. Exp. Phys. **2020** (2020) 083C01.
- [39] LHCb collaboration, R. Aaij *et al.*, *Measurement of CP observables in $B^\pm \rightarrow DK^\pm$ and $B^\pm \rightarrow D\pi^\pm$ with $D \rightarrow K_S^0 K^\pm \pi^\mp$ decays*, JHEP **06** (2020) 58, [arXiv:2002.08858](https://arxiv.org/abs/2002.08858).

LHCb collaboration

R. Aaij³², C. Abellán Beteta⁵⁰, T. Ackernley⁶⁰, B. Adeva⁴⁶, M. Adinolfi⁵⁴, H. Afsharnia⁹, C.A. Aidala⁸⁵, S. Aiola²⁵, Z. Ajaltouni⁹, S. Akar⁶⁵, J. Albrecht¹⁵, F. Alessio⁴⁸, M. Alexander⁵⁹, A. Alfonso Alberio⁴⁵, Z. Aliouche⁶², G. Alkhazov³⁸, P. Alvarez Cartelle⁵⁵, S. Amato², Y. Amhis¹¹, L. An⁴⁸, L. Anderlini²², A. Andreianov³⁸, M. Andreotti²¹, J.E. Andrews⁶⁶, F. Archilli¹⁷, A. Artamonov⁴⁴, M. Artuso⁶⁸, K. Arzymatov⁴², E. Aslanides¹⁰, M. Atzeni⁵⁰, B. Audurier¹², S. Bachmann¹⁷, M. Bachmayer⁴⁹, J.J. Back⁵⁶, S. Baker⁶¹, P. Baladron Rodriguez⁴⁶, V. Balagura¹², W. Baldini^{21,48}, J. Baptista Leite¹, R.J. Barlow⁶², S. Barsuk¹¹, W. Barter⁶¹, M. Bartolini^{24,g}, F. Baryshnikov⁸², J.M. Basels¹⁴, G. Bassi²⁹, B. Batsukh⁶⁸, A. Battig¹⁵, A. Bay⁴⁹, M. Becker¹⁵, F. Bedeschi²⁹, I. Bediaga¹, A. Beiter⁶⁸, V. Belavin⁴², S. Belin²⁷, V. Bellee⁴⁹, K. Belous⁴⁴, I. Belov⁴⁰, I. Belyaev⁴¹, G. Bencivenni²³, E. Ben-Haim¹³, A. Berezhnoy⁴⁰, R. Bernet⁵⁰, D. Berninghoff¹⁷, H.C. Bernstein⁶⁸, C. Bertella⁴⁸, E. Bertholet¹³, A. Bertolin²⁸, C. Betancourt⁵⁰, F. Betti^{20,c}, I.a. Bezshyiko⁵⁰, S. Bhasin⁵⁴, J. Bhom³⁵, L. Bian⁷³, M.S. Bieker¹⁵, S. Bifani⁵³, P. Billoir¹³, M. Birch⁶¹, F.C.R. Bishop⁵⁵, A. Bizzeti^{22,j}, M. Bjørn⁶³, M.P. Blago⁴⁸, T. Blake⁵⁶, F. Blanc⁴⁹, S. Blusk⁶⁸, D. Bobulska⁵⁹, J.A. Boelhauve¹⁵, O. Boente Garcia⁴⁶, T. Boettcher⁶⁴, A. Boldyrev⁸¹, A. Bondar⁴³, N. Bondar^{38,48}, S. Borghi⁶², M. Borisyak⁴², M. Borsato¹⁷, J.T. Borsuk³⁵, S.A. Bouchiba⁴⁹, T.J.V. Bowcock⁶⁰, A. Boyer⁴⁸, C. Bozzi²¹, M.J. Bradley⁶¹, S. Braun⁶⁶, A. Brea Rodriguez⁴⁶, M. Brodski⁴⁸, J. Brodzicka³⁵, A. Brossa Gonzalo⁵⁶, D. Brundu²⁷, A. Buonaura⁵⁰, C. Burr⁴⁸, A. Bursche²⁷, A. Butkevich³⁹, J.S. Butter³², J. Buytaert⁴⁸, W. Byczynski⁴⁸, S. Cadeddu²⁷, H. Cai⁷³, R. Calabrese^{21,e}, L. Calefice^{15,13}, L. Calero Diaz²³, S. Cali²³, R. Calladine⁵³, M. Calvi^{26,i}, M. Calvo Gomez⁸⁴, P. Camargo Magalhaes⁵⁴, A. Camboni^{45,84}, P. Campana²³, A.F. Campoverde Quezada⁶, S. Capelli^{26,i}, L. Capriotti^{20,c}, A. Carbone^{20,c}, G. Carboni³¹, R. Cardinale^{24,g}, A. Cardini²⁷, I. Carli⁴, P. Carniti^{26,i}, L. Carus¹⁴, K. Carvalho Akiba³², A. Casais Vidal⁴⁶, G. Casse⁶⁰, M. Cattaneo⁴⁸, G. Cavallero⁴⁸, S. Celani⁴⁹, J. Cerasoli¹⁰, A.J. Chadwick⁶⁰, M.G. Chapman⁵⁴, M. Charles¹³, Ph. Charpentier⁴⁸, G. Chatzikonstantinidis⁵³, C.A. Chavez Barajas⁶⁰, M. Chefdeville⁸, C. Chen³, S. Chen²⁷, A. Chernov³⁵, S.-G. Chitic⁴⁸, V. Chobanova⁴⁶, S. Cholak⁴⁹, M. Chrzaszcz³⁵, A. Chubykin³⁸, V. Chulikov³⁸, P. Ciambrone²³, M.F. Cicala⁵⁶, X. Cid Vidal⁴⁶, G. Ciezarek⁴⁸, P.E.L. Clarke⁵⁸, M. Clemencic⁴⁸, H.V. Cliff⁵⁵, J. Closier⁴⁸, J.L. Cobbledick⁶², V. Coco⁴⁸, J.A.B. Coelho¹¹, J. Cogan¹⁰, E. Cogneras⁹, L. Cojocariu³⁷, P. Collins⁴⁸, T. Colombo⁴⁸, L. Congedo^{19,b}, A. Contu²⁷, N. Cooke⁵³, G. Coombs⁵⁹, G. Corti⁴⁸, C.M. Costa Sobral⁵⁶, B. Couturier⁴⁸, D.C. Craik⁶⁴, J. Crkovašá⁶⁷, M. Cruz Torres¹, R. Currie⁵⁸, C.L. Da Silva⁶⁷, E. Dall'Occo¹⁵, J. Dalseno⁴⁶, C. D'Ambrosio⁴⁸, A. Danilina⁴¹, P. d'Argent⁴⁸, A. Davis⁶², O. De Aguiar Francisco⁶², K. De Bruyn⁷⁸, S. De Capua⁶², M. De Cian⁴⁹, J.M. De Miranda¹, L. De Paula², M. De Serio^{19,b}, D. De Simone⁵⁰, P. De Simone²³, J.A. de Vries⁷⁹, C.T. Dean⁶⁷, W. Dean⁸⁵, D. Decamp⁸, L. Del Buono¹³, B. Delaney⁵⁵, H.-P. Dembinski¹⁵, A. Dendek³⁴, V. Denysenko⁵⁰, D. Derkach⁸¹, O. Deschamps⁹, F. Dese¹¹, F. Dettori^{27,d}, B. Dey⁷³, P. Di Nezza²³, S. Didenko⁸², L. Dieste Maronas⁴⁶, H. Dijkstra⁴⁸, V. Dobishuk⁵², A.M. Donohoe¹⁸, F. Dordei²⁷, A.C. dos Reis¹, L. Douglas⁵⁹, A. Dovbnya⁵¹, A.G. Downes⁸, K. Dreimanis⁶⁰, M.W. Dudek³⁵, L. Dufour⁴⁸, V. Duk⁷⁷, P. Durante⁴⁸, J.M. Durham⁶⁷, D. Dutta⁶², M. Dziewiecki¹⁷, A. Dziurda³⁵, A. Dzyuba³⁸, S. Easo⁵⁷, U. Egede⁶⁹, V. Egorychev⁴¹, S. Eidelman^{43,u}, S. Eisenhardt⁵⁸, S. Ek-In⁴⁹, L. Eklund⁵⁹, S. Ely⁶⁸, A. Ene³⁷, E. Epple⁶⁷, S. Escher¹⁴, J. Eschle⁵⁰, S. Esen³², T. Evans⁴⁸, A. Falabella²⁰, J. Fan³, Y. Fan⁶, B. Fang⁷³, N. Farley⁵³, S. Farry⁶⁰, D. Fazzini^{26,i}, P. Fedin⁴¹, M. Féo⁴⁸, P. Fernandez Declara⁴⁸, A. Fernandez Prieto⁴⁶, J.M. Fernandez-tenllado Arribas⁴⁵, F. Ferrari^{20,c}, L. Ferreira Lopes⁴⁹, F. Ferreira Rodrigues², S. Ferreres Sole³², M. Ferrillo⁵⁰, M. Ferro-Luzzi⁴⁸, S. Filippov³⁹, R.A. Fini¹⁹, M. Fiorini^{21,e}, M. Firlej³⁴, K.M. Fischer⁶³, C. Fitzpatrick⁶², T. Fiutowski³⁴, F. Fleuret¹², M. Fontana¹³, F. Fontanelli^{24,g}, R. Forty⁴⁸, V. Franco Lima⁶⁰, M. Franco Sevilla⁶⁶, M. Frank⁴⁸, E. Franzoso²¹,

G. Frau¹⁷, C. Frei⁴⁸, D.A. Friday⁵⁹, J. Fu²⁵, Q. Fuehring¹⁵, W. Funk⁴⁸, E. Gabriel³²,
 T. Gaintseva⁴², A. Gallas Torreira⁴⁶, D. Galli^{20,c}, S. Gambetta^{58,48}, Y. Gan³, M. Gandelman²,
 P. Gandini²⁵, Y. Gao⁵, M. Garau²⁷, L.M. Garcia Martin⁵⁶, P. Garcia Moreno⁴⁵,
 J. García Pardiñas²⁶, B. Garcia Plana⁴⁶, F.A. Garcia Rosales¹², L. Garrido⁴⁵, C. Gaspar⁴⁸,
 R.E. Geertsema³², D. Gerick¹⁷, L.L. Gerken¹⁵, E. Gersabeck⁶², M. Gersabeck⁶², T. Gershon⁵⁶,
 D. Gerstel¹⁰, Ph. Ghez⁸, V. Gibson⁵⁵, M. Giovannetti^{23,o}, A. Gioventù⁴⁶,
 P. Gironella Gironell⁴⁵, L. Giubega³⁷, C. Giugliano^{21,e,48}, K. Gizdov⁵⁸, E.L. Gkougkousis⁴⁸,
 V.V. Gligorov¹³, C. Göbel⁷⁰, E. Golobardes⁸⁴, D. Golubkov⁴¹, A. Golutvin^{61,82}, A. Gomes^{1,a},
 S. Gomez Fernandez⁴⁵, F. Goncalves Abrantes⁷⁰, M. Goncerz³⁵, G. Gong³, P. Gorbounov⁴¹,
 I.V. Gorelov⁴⁰, C. Gotti²⁶, E. Govorkova⁴⁸, J.P. Grabowski¹⁷, R. Graciani Diaz⁴⁵,
 T. Grammatico¹³, L.A. Granado Cardoso⁴⁸, E. Graugés⁴⁵, E. Graverini⁴⁹, G. Graziani²²,
 A. Grecu³⁷, L.M. Greeven³², P. Griffith^{21,e}, L. Grillo⁶², S. Gromov⁸², B.R. Gruberg Cazon⁶³,
 C. Gu³, M. Guarise²¹, P. A. Günther¹⁷, E. Gushchin³⁹, A. Guth¹⁴, Y. Guz^{44,48}, T. Gys⁴⁸,
 T. Hadavizadeh⁶⁹, G. Haefeli⁴⁹, C. Haen⁴⁸, J. Haimberger⁴⁸, T. Halewood-leagas⁶⁰,
 P.M. Hamilton⁶⁶, Q. Han⁷, X. Han¹⁷, T.H. Hancock⁶³, S. Hansmann-Menzemer¹⁷, N. Harnew⁶³,
 T. Harrison⁶⁰, C. Hasse⁴⁸, M. Hatch⁴⁸, J. He⁶, M. Hecker⁶¹, K. Heijhoff³², K. Heinicke¹⁵,
 A.M. Hennequin⁴⁸, K. Hennessy⁶⁰, L. Henry^{25,47}, J. Heuel¹⁴, A. Hicheur², D. Hill⁴⁹, M. Hilton⁶²,
 S.E. Hollitt¹⁵, J. Hu¹⁷, J. Hu⁷², W. Hu⁷, W. Huang⁶, X. Huang⁷³, W. Hulsbergen³²,
 R.J. Hunter⁵⁶, M. Hushchyn⁸¹, D. Hutchcroft⁶⁰, D. Hynds³², P. Ibis¹⁵, M. Idzik³⁴, D. Ilin³⁸,
 P. Ilten⁶⁵, A. Inglessi³⁸, A. Ishteev⁸², K. Ivshin³⁸, R. Jacobsson⁴⁸, S. Jakobsen⁴⁸, E. Jans³²,
 B.K. Jashal⁴⁷, A. Jawahery⁶⁶, V. Jevtic¹⁵, M. Jezabek³⁵, F. Jiang³, M. John⁶³, D. Johnson⁴⁸,
 C.R. Jones⁵⁵, T.P. Jones⁵⁶, B. Jost⁴⁸, N. Jurik⁴⁸, S. Kandybei⁵¹, Y. Kang³, M. Karacson⁴⁸,
 M. Karpov⁸¹, N. Kazeev⁸¹, F. Keizer^{55,48}, M. Kenzie⁵⁶, T. Ketel³³, B. Khanji¹⁵, A. Kharisova⁸³,
 S. Kholodenko⁴⁴, K.E. Kim⁶⁸, T. Kirn¹⁴, V.S. Kirsebom⁴⁹, O. Kitouni⁶⁴, S. Klaver³²,
 K. Klimaszewski³⁶, S. Koliiev⁵², A. Kondybayeva⁸², A. Konoplyannikov⁴¹, P. Kopciwicz³⁴,
 R. Kopečna¹⁷, P. Koppenburg³², M. Korolev⁴⁰, I. Kostiuk^{32,52}, O. Kot⁵², S. Kotriakhova^{38,30},
 P. Kravchenko³⁸, L. Kravchuk³⁹, R.D. Krawczyk⁴⁸, M. Kreps⁵⁶, F. Kress⁶¹, S. Kretzschmar¹⁴,
 P. Krokovny^{43,u}, W. Krupa³⁴, W. Krzemien³⁶, W. Kucewicz^{35,s}, M. Kucharczyk³⁵,
 V. Kudryavtsev^{43,u}, H.S. Kuindersma³², G.J. Kunde⁶⁷, T. Kvaratskheliya⁴¹, D. Lacarrere⁴⁸,
 G. Lafferty⁶², A. Lai²⁷, A. Lampis²⁷, D. Lancierini⁵⁰, J.J. Lane⁶², R. Lane⁵⁴, G. Lanfranchi²³,
 C. Langenbruch¹⁴, J. Langer¹⁵, O. Lantwin^{50,82}, T. Latham⁵⁶, F. Lazzari^{29,p}, R. Le Gac¹⁰,
 S.H. Lee⁸⁵, R. Lefèvre⁹, A. Leflat⁴⁰, S. Legotin⁸², O. Leroy¹⁰, T. Lesiak³⁵, B. Leverington¹⁷,
 H. Li⁷², L. Li⁶³, P. Li¹⁷, Y. Li⁴, Y. Li⁴, Z. Li⁶⁸, X. Liang⁶⁸, T. Lin⁶¹, R. Lindner⁴⁸,
 V. Lisovskyi¹⁵, R. Litvinov²⁷, G. Liu⁷², H. Liu⁶, S. Liu⁴, X. Liu³, A. Loi²⁷, J. Lomba Castro⁴⁶,
 I. Longstaff⁵⁹, J.H. Lopes², G. Loustau⁵⁰, G.H. Lovell⁵⁵, Y. Lu⁴, D. Lucchesi^{28,k}, S. Luchuk³⁹,
 M. Lucio Martinez³², V. Lukashenko³², Y. Luo³, A. Lupato⁶², E. Luppi^{21,e}, O. Lupton⁵⁶,
 A. Lusiani^{29,l}, X. Lyu⁶, L. Ma⁴, R. Ma⁶, S. Maccolini^{20,c}, F. Machefer¹¹, F. Maciuc³⁷,
 V. Macko⁴⁹, P. Mackowiak¹⁵, S. Maddrell-Mander⁵⁴, O. Madejczyk³⁴, L.R. Madhan Mohan⁵⁴,
 O. Maev³⁸, A. Maevskiy⁸¹, D. Maisuzenko³⁸, M.W. Majewski³⁴, J.J. Malczewski³⁵, S. Malde⁶³,
 B. Malecki⁴⁸, A. Malinin⁸⁰, T. Maltsev^{43,u}, H. Malygina¹⁷, G. Manca^{27,d}, G. Mancinelli¹⁰,
 R. Manera Escalero⁴⁵, D. Manuzzi^{20,c}, D. Marangotto^{25,h}, J. Maratas^{9,r}, J.F. Marchand⁸,
 U. Marconi²⁰, S. Mariani^{22,f,48}, C. Marin Benito¹¹, M. Marinangeli⁴⁹, P. Marino^{49,l}, J. Marks¹⁷,
 P.J. Marshall⁶⁰, G. Martellotti³⁰, L. Martinazzoli^{48,i}, M. Martinelli^{26,i}, D. Martinez Santos⁴⁶,
 F. Martinez Vidal⁴⁷, A. Massafferri¹, M. Materok¹⁴, R. Matev⁴⁸, A. Mathad⁵⁰, Z. Mathe⁴⁸,
 V. Matiunin⁴¹, C. Matteuzzi²⁶, K.R. Mattioli⁸⁵, A. Mauri³², E. Maurice¹², J. Mauricio⁴⁵,
 M. Mazurek³⁶, M. McCann⁶¹, L. Mcconnell¹⁸, T.H. Mcgrath⁶², A. McNab⁶², R. McNulty¹⁸,
 J.V. Mead⁶⁰, B. Meadows⁶⁵, C. Meaux¹⁰, G. Meier¹⁵, N. Meinert⁷⁶, D. Melnychuk³⁶,
 S. Meloni^{26,i}, M. Merk^{32,79}, A. Merli²⁵, L. Meyer Garcia², M. Mikhasenko⁴⁸, D.A. Milanese⁷⁴,
 E. Millard⁵⁶, M. Milovanovic⁴⁸, M.-N. Minard⁸, L. Minzoni^{21,e}, S.E. Mitchell⁵⁸, B. Mitreska⁶²,
 D.S. Mitzel⁴⁸, A. Mödden¹⁵, R.A. Mohammed⁶³, R.D. Moise⁶¹, T. Mombächer¹⁵,

I.A. Monroy⁷⁴, S. Monteil⁹, M. Morandin²⁸, G. Morello²³, M.J. Morello^{29,l}, J. Moron³⁴,
 A.B. Morris⁷⁵, A.G. Morris⁵⁶, R. Mountain⁶⁸, H. Mu³, F. Muheim⁵⁸, M. Mukherjee⁷,
 M. Mulder⁴⁸, D. Müller⁴⁸, K. Müller⁵⁰, C.H. Murphy⁶³, D. Murray⁶², P. Muzzetto^{27,48},
 P. Naik⁵⁴, T. Nakada⁴⁹, R. Nandakumar⁵⁷, T. Nanut⁴⁹, I. Nasteva², M. Needham⁵⁸, I. Neri^{21,e},
 N. Neri^{25,h}, S. Neubert⁷⁵, N. Neufeld⁴⁸, R. Newcombe⁶¹, T.D. Nguyen⁴⁹, C. Nguyen-Mau^{49,v},
 E.M. Niel¹¹, S. Nieswand¹⁴, N. Nikitin⁴⁰, N.S. Nolte⁴⁸, C. Nunez⁸⁵, A. Oblakowska-Mucha³⁴,
 V. Obraztsov⁴⁴, D.P. O'Hanlon⁵⁴, R. Oldeman^{27,d}, M.E. Olivares⁶⁸, C.J.G. Onderwater⁷⁸,
 A. Ossowska³⁵, J.M. Otalora Goicochea², T. Ovsiannikova⁴¹, P. Owen⁵⁰, A. Oyanguren⁴⁷,
 B. Pagare⁵⁶, P.R. Pais⁴⁸, T. Pajero^{29,l,48}, A. Palano¹⁹, M. Palutan²³, Y. Pan⁶², G. Panshin⁸³,
 A. Papanestis⁵⁷, M. Pappagallo^{19,b}, L.L. Pappalardo^{21,e}, C. Pappenheimer⁶⁵, W. Parker⁶⁶,
 C. Parkes⁶², C.J. Parkinson⁴⁶, B. Passalacqua²¹, G. Passaleva²², A. Pastore¹⁹, M. Patel⁶¹,
 C. Patrignani^{20,c}, C.J. Pawley⁷⁹, A. Pearce⁴⁸, A. Pellegrino³², M. Pepe Altarelli⁴⁸,
 S. Perazzini²⁰, D. Pereima⁴¹, P. Perret⁹, K. Petridis⁵⁴, A. Petrolini^{24,g}, A. Petrov⁸⁰,
 S. Petrucci⁵⁸, M. Petruzzo²⁵, T.T.H. Pham⁶⁸, A. Philippov⁴², L. Pica²⁹, M. Piccini⁷⁷,
 B. Pietrzyk⁸, G. Pietrzyk⁴⁹, M. Pili⁶³, D. Pinci³⁰, F. Pisani⁴⁸, A. Piucci¹⁷, Resmi P.K¹⁰,
 V. Placinta³⁷, J. Plews⁵³, M. Plo Casasus⁴⁶, F. Polci¹³, M. Poli Lener²³, M. Poliakova⁶⁸,
 A. Poluektov¹⁰, N. Polukhina^{82,t}, I. Polyakov⁶⁸, E. Polcarpo², G.J. Pomery⁵⁴, S. Ponce⁴⁸,
 D. Popov^{6,48}, S. Popov⁴², S. Poslavskii⁴⁴, K. Prasanth³⁵, L. Promberger⁴⁸, C. Prouve⁴⁶,
 V. Pugatch⁵², H. Pullen⁶³, G. Punzi^{29,m}, W. Qian⁶, J. Qin⁶, R. Quagliani¹³, B. Quintana⁸,
 N.V. Raab¹⁸, R.I. Rabadan Trejo¹⁰, B. Rachwal³⁴, J.H. Rademacker⁵⁴, M. Rama²⁹,
 M. Ramos Pernas⁵⁶, M.S. Rangel², F. Ratnikov^{42,81}, G. Raven³³, M. Reboud⁸, F. Redi⁴⁹,
 F. Reiss¹³, C. Remon Alepuz⁴⁷, Z. Ren³, V. Renaudin⁶³, R. Ribatti²⁹, S. Ricciardi⁵⁷,
 K. Rinnert⁶⁰, P. Robbe¹¹, A. Robert¹³, G. Robertson⁵⁸, A.B. Rodrigues⁴⁹, E. Rodrigues⁶⁰,
 J.A. Rodriguez Lopez⁷⁴, A. Rollings⁶³, P. Roloff⁴⁸, V. Romanovskiy⁴⁴, M. Romero Lamas⁴⁶,
 A. Romero Vidal⁴⁶, J.D. Roth⁸⁵, M. Rotondo²³, M.S. Rudolph⁶⁸, T. Ruf⁴⁸, J. Ruiz Vidal⁴⁷,
 A. Ryzhikov⁸¹, J. Ryzka³⁴, J.J. Saborido Silva⁴⁶, N. Sagidova³⁸, N. Sahoo⁵⁶, B. Saitta^{27,d},
 D. Sanchez Gonzalo⁴⁵, C. Sanchez Gras³², R. Santacesaria³⁰, C. Santamarina Rios⁴⁶,
 M. Santimaria²³, E. Santovetti^{31,o}, D. Saranin⁸², G. Sarpis⁵⁹, M. Sarpis⁷⁵, A. Sarti³⁰,
 C. Satriano^{30,n}, A. Satta³¹, M. Saur¹⁵, D. Savrina^{41,40}, H. Sazak⁹, L.G. Scantlebury Smead⁶³,
 S. Schael¹⁴, M. Schellenberg¹⁵, M. Schiller⁵⁹, H. Schindler⁴⁸, M. Schmelling¹⁶, B. Schmidt⁴⁸,
 O. Schneider⁴⁹, A. Schopper⁴⁸, M. Schubiger³², S. Schulte⁴⁹, M.H. Schune¹¹, R. Schwemmer⁴⁸,
 B. Sciascia²³, A. Sciubba²³, S. Sellam⁴⁶, A. Semennikov⁴¹, M. Senghi Soares³³, A. Sergi^{53,48},
 N. Serra⁵⁰, L. Sestini²⁸, A. Seuthe¹⁵, P. Seyfert⁴⁸, D.M. Shangase⁸⁵, M. Shapkin⁴⁴,
 I. Shchemerov⁸², L. Shchutska⁴⁹, T. Shears⁶⁰, L. Shekhtman^{43,u}, Z. Shen⁵, V. Shevchenko⁸⁰,
 E.B. Shields^{26,i}, E. Shmanin⁸², J.D. Shupperd⁶⁸, B.G. Siddi²¹, R. Silva Coutinho⁵⁰, G. Simi²⁸,
 S. Simone^{19,b}, I. Skiba^{21,e}, N. Skidmore⁶², T. Skwarnicki⁶⁸, M.W. Slater⁵³, J.C. Smallwood⁶³,
 J.G. Smeaton⁵⁵, A. Smetkina⁴¹, E. Smith¹⁴, M. Smith⁶¹, A. Snoch³², M. Soares²⁰,
 L. Soares Lavra⁹, M.D. Sokoloff⁶⁵, F.J.P. Soler⁵⁹, A. Solovov³⁸, I. Solovyevev³⁸,
 F.L. Souza De Almeida², B. Souza De Paula², B. Spaan¹⁵, E. Spadaro Norella^{25,h}, P. Spradlin⁵⁹,
 F. Stagni⁴⁸, M. Stahl⁶⁵, S. Stahl⁴⁸, P. Stefko⁴⁹, O. Steinkamp^{50,82}, S. Stemmler¹⁷,
 O. Stenyakin⁴⁴, H. Stevens¹⁵, S. Stone⁶⁸, M.E. Stramaglia⁴⁹, M. Straticiu³⁷, D. Strelakina⁸²,
 S. Strovkov⁸³, F. Suljik⁶³, J. Sun²⁷, L. Sun⁷³, Y. Sun⁶⁶, P. Svihra⁶², P.N. Swallow⁵³,
 K. Swientek³⁴, A. Szabelski³⁶, T. Szumlak³⁴, M. Szymanski⁴⁸, S. Taneja⁶², F. Teubert⁴⁸,
 E. Thomas⁴⁸, K.A. Thomson⁶⁰, M.J. Tilley⁶¹, V. Tisserand⁹, S. T'Jampens⁸, M. Tobin⁴,
 S. Tolk⁴⁸, L. Tomassetti^{21,e}, D. Torres Machado¹, D.Y. Tou¹³, M. Traill⁵⁹, M.T. Tran⁴⁹,
 E. Trifonova⁸², C. Trippi⁴⁹, G. Tuci^{29,m}, A. Tully⁴⁹, N. Tuning³², A. Ukleja³⁶, D.J. Unverzagt¹⁷,
 E. Ursov⁸², A. Usachov³², A. Ustyuzhanin^{42,81}, U. Uwer¹⁷, A. Vagner⁸³, V. Vagnoni²⁰,
 A. Valassi⁴⁸, G. Valenti²⁰, N. Valls Canudas⁴⁵, M. van Beuzekom³², M. Van Dijk⁴⁹,
 E. van Herwijnen⁸², C.B. Van Hulse¹⁸, M. van Veghel⁷⁸, R. Vazquez Gomez⁴⁶,
 P. Vazquez Regueiro⁴⁶, C. Vázquez Sierra⁴⁸, S. Vecchi²¹, J.J. Velthuis⁵⁴, M. Veltri^{22,q},

A. Venkateswaran⁶⁸, M. Veronesi³², M. Vesterinen⁵⁶, D. Vieira⁶⁵, M. Vieites Diaz⁴⁹, H. Viemann⁷⁶, X. Vilasis-Cardona⁸⁴, E. Vilella Figueras⁶⁰, P. Vincent¹³, G. Vitali²⁹, A. Vollhardt⁵⁰, D. Vom Bruch¹³, A. Vorobyev³⁸, V. Vorobyev^{43,u}, N. Voropaev³⁸, R. Waldi⁷⁶, J. Walsh²⁹, C. Wang¹⁷, J. Wang⁵, J. Wang⁴, J. Wang³, J. Wang⁷³, M. Wang³, R. Wang⁵⁴, Y. Wang⁷, Z. Wang⁵⁰, H.M. Wark⁶⁰, N.K. Watson⁵³, S.G. Weber¹³, D. Websdale⁶¹, C. Weisser⁶⁴, B.D.C. Westhenry⁵⁴, D.J. White⁶², M. Whitehead⁵⁴, D. Wiedner¹⁵, G. Wilkinson⁶³, M. Wilkinson⁶⁸, I. Williams⁵⁵, M. Williams^{64,69}, M.R.J. Williams⁵⁸, F.F. Wilson⁵⁷, W. Wislicki³⁶, M. Witek³⁵, L. Witola¹⁷, G. Wormser¹¹, S.A. Wotton⁵⁵, H. Wu⁶⁸, K. Wyllie⁴⁸, Z. Xiang⁶, D. Xiao⁷, Y. Xie⁷, A. Xu⁵, J. Xu⁶, L. Xu³, M. Xu⁷, Q. Xu⁶, Z. Xu⁵, Z. Xu⁶, D. Yang³, S. Yang⁶, Y. Yang⁶, Z. Yang³, Z. Yang⁶⁶, Y. Yao⁶⁸, L.E. Yeomans⁶⁰, H. Yin⁷, J. Yu⁷¹, X. Yuan⁶⁸, O. Yushchenko⁴⁴, E. Zaffaroni⁴⁹, K.A. Zarebski⁵³, M. Zavertyaev^{16,t}, M. Zdybal³⁵, O. Zenaiev⁴⁸, M. Zeng³, D. Zhang⁷, L. Zhang³, S. Zhang⁵, Y. Zhang⁵, Y. Zhang⁶³, A. Zhelezov¹⁷, Y. Zheng⁶, X. Zhou⁶, Y. Zhou⁶, X. Zhu³, V. Zhukov^{14,40}, J.B. Zonneveld⁵⁸, S. Zucchelli^{20,c}, D. Zuliani²⁸, G. Zunica⁶².

¹ *Centro Brasileiro de Pesquisas Físicas (CBPF), Rio de Janeiro, Brazil*

² *Universidade Federal do Rio de Janeiro (UFRJ), Rio de Janeiro, Brazil*

³ *Center for High Energy Physics, Tsinghua University, Beijing, China*

⁴ *Institute Of High Energy Physics (IHEP), Beijing, China*

⁵ *School of Physics State Key Laboratory of Nuclear Physics and Technology, Peking University, Beijing, China*

⁶ *University of Chinese Academy of Sciences, Beijing, China*

⁷ *Institute of Particle Physics, Central China Normal University, Wuhan, Hubei, China*

⁸ *Univ. Grenoble Alpes, Univ. Savoie Mont Blanc, CNRS, IN2P3-LAPP, Annecy, France*

⁹ *Université Clermont Auvergne, CNRS/IN2P3, LPC, Clermont-Ferrand, France*

¹⁰ *Aix Marseille Univ, CNRS/IN2P3, CPPM, Marseille, France*

¹¹ *Université Paris-Saclay, CNRS/IN2P3, IJCLab, Orsay, France*

¹² *Laboratoire Leprince-ringuet (lir), Palaiseau, France*

¹³ *LPNHE, Sorbonne Université, Paris Diderot Sorbonne Paris Cité, CNRS/IN2P3, Paris, France*

¹⁴ *I. Physikalisches Institut, RWTH Aachen University, Aachen, Germany*

¹⁵ *Fakultät Physik, Technische Universität Dortmund, Dortmund, Germany*

¹⁶ *Max-Planck-Institut für Kernphysik (MPIK), Heidelberg, Germany*

¹⁷ *Physikalisches Institut, Ruprecht-Karls-Universität Heidelberg, Heidelberg, Germany*

¹⁸ *School of Physics, University College Dublin, Dublin, Ireland*

¹⁹ *INFN Sezione di Bari, Bari, Italy*

²⁰ *INFN Sezione di Bologna, Bologna, Italy*

²¹ *INFN Sezione di Ferrara, Ferrara, Italy*

²² *INFN Sezione di Firenze, Firenze, Italy*

²³ *INFN Laboratori Nazionali di Frascati, Frascati, Italy*

²⁴ *INFN Sezione di Genova, Genova, Italy*

²⁵ *INFN Sezione di Milano, Milano, Italy*

²⁶ *INFN Sezione di Milano-Bicocca, Milano, Italy*

²⁷ *INFN Sezione di Cagliari, Monserrato, Italy*

²⁸ *Università degli Studi di Padova, Università e INFN, Padova, Padova, Italy*

²⁹ *INFN Sezione di Pisa, Pisa, Italy*

³⁰ *INFN Sezione di Roma La Sapienza, Roma, Italy*

³¹ *INFN Sezione di Roma Tor Vergata, Roma, Italy*

³² *Nikhef National Institute for Subatomic Physics, Amsterdam, Netherlands*

³³ *Nikhef National Institute for Subatomic Physics and VU University Amsterdam, Amsterdam, Netherlands*

³⁴ *AGH - University of Science and Technology, Faculty of Physics and Applied Computer Science, Kraków, Poland*

³⁵ *Henryk Niewodniczanski Institute of Nuclear Physics Polish Academy of Sciences, Kraków, Poland*

³⁶ *National Center for Nuclear Research (NCBJ), Warsaw, Poland*

³⁷ *Horia Hulubei National Institute of Physics and Nuclear Engineering, Bucharest-Magurele, Romania*

- ³⁸ Petersburg Nuclear Physics Institute NRC Kurchatov Institute (PNPI NRC KI), Gatchina, Russia
- ³⁹ Institute for Nuclear Research of the Russian Academy of Sciences (INR RAS), Moscow, Russia
- ⁴⁰ Institute of Nuclear Physics, Moscow State University (SINP MSU), Moscow, Russia
- ⁴¹ Institute of Theoretical and Experimental Physics NRC Kurchatov Institute (ITEP NRC KI), Moscow, Russia
- ⁴² Yandex School of Data Analysis, Moscow, Russia
- ⁴³ Budker Institute of Nuclear Physics (SB RAS), Novosibirsk, Russia
- ⁴⁴ Institute for High Energy Physics NRC Kurchatov Institute (IHEP NRC KI), Protvino, Russia, Protvino, Russia
- ⁴⁵ ICCUB, Universitat de Barcelona, Barcelona, Spain
- ⁴⁶ Instituto Galego de Física de Altas Enerxías (IGFAE), Universidade de Santiago de Compostela, Santiago de Compostela, Spain
- ⁴⁷ Instituto de Física Corpuscular, Centro Mixto Universidad de Valencia - CSIC, Valencia, Spain
- ⁴⁸ European Organization for Nuclear Research (CERN), Geneva, Switzerland
- ⁴⁹ Institute of Physics, Ecole Polytechnique Fédérale de Lausanne (EPFL), Lausanne, Switzerland
- ⁵⁰ Physik-Institut, Universität Zürich, Zürich, Switzerland
- ⁵¹ NSC Kharkiv Institute of Physics and Technology (NSC KIPT), Kharkiv, Ukraine
- ⁵² Institute for Nuclear Research of the National Academy of Sciences (KINR), Kyiv, Ukraine
- ⁵³ University of Birmingham, Birmingham, United Kingdom
- ⁵⁴ H.H. Wills Physics Laboratory, University of Bristol, Bristol, United Kingdom
- ⁵⁵ Cavendish Laboratory, University of Cambridge, Cambridge, United Kingdom
- ⁵⁶ Department of Physics, University of Warwick, Coventry, United Kingdom
- ⁵⁷ STFC Rutherford Appleton Laboratory, Didcot, United Kingdom
- ⁵⁸ School of Physics and Astronomy, University of Edinburgh, Edinburgh, United Kingdom
- ⁵⁹ School of Physics and Astronomy, University of Glasgow, Glasgow, United Kingdom
- ⁶⁰ Oliver Lodge Laboratory, University of Liverpool, Liverpool, United Kingdom
- ⁶¹ Imperial College London, London, United Kingdom
- ⁶² Department of Physics and Astronomy, University of Manchester, Manchester, United Kingdom
- ⁶³ Department of Physics, University of Oxford, Oxford, United Kingdom
- ⁶⁴ Massachusetts Institute of Technology, Cambridge, MA, United States
- ⁶⁵ University of Cincinnati, Cincinnati, OH, United States
- ⁶⁶ University of Maryland, College Park, MD, United States
- ⁶⁷ Los Alamos National Laboratory (LANL), Los Alamos, United States
- ⁶⁸ Syracuse University, Syracuse, NY, United States
- ⁶⁹ School of Physics and Astronomy, Monash University, Melbourne, Australia, associated to ⁵⁶
- ⁷⁰ Pontifícia Universidade Católica do Rio de Janeiro (PUC-Rio), Rio de Janeiro, Brazil, associated to ²
- ⁷¹ Physics and Micro Electronic College, Hunan University, Changsha City, China, associated to ⁷
- ⁷² Guangdong Provincial Key Laboratory of Nuclear Science, Institute of Quantum Matter, South China Normal University, Guangzhou, China, associated to ³
- ⁷³ School of Physics and Technology, Wuhan University, Wuhan, China, associated to ³
- ⁷⁴ Departamento de Física, Universidad Nacional de Colombia, Bogota, Colombia, associated to ¹³
- ⁷⁵ Universität Bonn - Helmholtz-Institut für Strahlen und Kernphysik, Bonn, Germany, associated to ¹⁷
- ⁷⁶ Institut für Physik, Universität Rostock, Rostock, Germany, associated to ¹⁷
- ⁷⁷ INFN Sezione di Perugia, Perugia, Italy, associated to ²¹
- ⁷⁸ Van Swinderen Institute, University of Groningen, Groningen, Netherlands, associated to ³²
- ⁷⁹ Universiteit Maastricht, Maastricht, Netherlands, associated to ³²
- ⁸⁰ National Research Centre Kurchatov Institute, Moscow, Russia, associated to ⁴¹
- ⁸¹ National Research University Higher School of Economics, Moscow, Russia, associated to ⁴²
- ⁸² National University of Science and Technology "MISIS", Moscow, Russia, associated to ⁴¹
- ⁸³ National Research Tomsk Polytechnic University, Tomsk, Russia, associated to ⁴¹
- ⁸⁴ DS4DS, La Salle, Universitat Ramon Llull, Barcelona, Spain, associated to ⁴⁵
- ⁸⁵ University of Michigan, Ann Arbor, United States, associated to ⁶⁸

^a Universidade Federal do Triângulo Mineiro (UFTM), Uberaba-MG, Brazil

^b Università di Bari, Bari, Italy

^c Università di Bologna, Bologna, Italy

^d Università di Cagliari, Cagliari, Italy

- ^e *Università di Ferrara, Ferrara, Italy*
- ^f *Università di Firenze, Firenze, Italy*
- ^g *Università di Genova, Genova, Italy*
- ^h *Università degli Studi di Milano, Milano, Italy*
- ⁱ *Università di Milano Bicocca, Milano, Italy*
- ^j *Università di Modena e Reggio Emilia, Modena, Italy*
- ^k *Università di Padova, Padova, Italy*
- ^l *Scuola Normale Superiore, Pisa, Italy*
- ^m *Università di Pisa, Pisa, Italy*
- ⁿ *Università della Basilicata, Potenza, Italy*
- ^o *Università di Roma Tor Vergata, Roma, Italy*
- ^p *Università di Siena, Siena, Italy*
- ^q *Università di Urbino, Urbino, Italy*
- ^r *MSU - Iligan Institute of Technology (MSU-IIT), Iligan, Philippines*
- ^s *AGH - University of Science and Technology, Faculty of Computer Science, Electronics and Telecommunications, Kraków, Poland*
- ^t *P.N. Lebedev Physical Institute, Russian Academy of Science (LPI RAS), Moscow, Russia*
- ^u *Novosibirsk State University, Novosibirsk, Russia*
- ^v *Hanoi University of Science, Hanoi, Vietnam*